University of Milan

Faculty of Political, Economic and Social Sciences

A Bayesian Approach to Aggregate Insurance Claim Modeling

Final Project in the Subject Bayesian Analysis

Julia Maria Wdowinska (43288A)
Edoardo Zanone (33927A)

Data Science for Economics
II Year
Master's Degree

April 29, 2025

Contents

1 Introduction

2 Theoretical Background

In insurance modeling, accurately estimating the aggregate value of claims is essential for premium calculation, risk assessment, and maintaining solvency of insurance providers. The aggregate claim value refers to the total amount paid out for claims over a specified period. This quantity is typically modeled using a compound distribution, which separately describes the frequency and severity of claims. The frequency component, representing the number of claims within the period, is often modeled using a Poisson distribution. The severity component, which captures the magnitude of individual claims, is commonly modeled using heavy-tailed distributions such as the Pareto or Gamma distributions.

The traditional framework for modeling such processes is grounded in frequentist statistics. In this approach, the parameters of the underlying distributions—such as the Poisson rate parameter λ, or the shape and scale parameters α and β of the Pareto distribution—are considered fixed but unknown quantities. These parameters are typically estimated from observed data using techniques such as maximum likelihood estimation (MLE).

In contrast, the Bayesian framework treats these parameters as random variables characterized by prior distributions. This allows for the incorporation of prior knowledge or beliefs about the parameters before any data is observed. The prior distribution is updated using Bayes' theorem upon observing data, resulting in a posterior distribution that reflects the updated beliefs. This posterior distribution forms the basis for inference and prediction.

Bayesian methods offer significant advantages in insurance modeling. They are well-suited for incorporating expert knowledge or external information, handling limited or noisy datasets, and accommodating complex hierarchical structures commonly found in insurance data. Moreover, Bayesian inference provides a coherent framework for uncertainty quantification by yielding full posterior distributions over model parameters.

Nevertheless, Bayesian methods also come with certain limitations. The choice of prior distribution can introduce subjectivity, and computational complexity can be significant, especially in models with high dimensionality or non-conjugate priors. Despite these challenges, the flexibility and robustness of the Bayesian framework make it a valuable approach for modeling aggregate insurance claims.

3 Replication of Dudley (2006)

Building on the theoretical background, this project aims to replicate the Bayesian modeling approach proposed by Dudley (2006). The analysis is based on a dataset of automobile insurance claims exceeding 1.5 million, collected over a five-year period. The data, originally reported by Rytgaard (1990), is presented in Table 1.

Table 1: Insurance Claim Amounts Exceeding 1.5 Million (Data from Rytgaard, 1990)

Year	**Claim Amounts (in millions)**				
1	2.495	2.120	2.095	1.700	1.650
2	1.985	1.810	1.625	–	–
3	3.215	2.105	1.765	1.715	–
4	–	–	–	–	–
5	19.180	1.915	1.790	1.755	–

The threshold of 1.5 million corresponds to the retention level of an excess-of-loss insurance policy[1].

[1] To manage risk exposure, insurers frequently employ reinsurance strategies, which help reduce their financial liability on large claims. Under such arrangements, if a claim amount y exceeds a predetermined threshold d (the retention), the insurer is responsible only for paying up to d, while any excess $y - d$ is covered by the reinsurer.

3.1 Model Specification

To model this dataset within a Bayesian framework, assumptions about the distributions of both the number of claims in year t (N_t) and the amount of the i-th claim in year t ($Y_{i,t}$) were necessary. Claims were assumed to occur randomly and independently at a constant rate over time, so N_t was modeled using a Poisson distribution. A Pareto distribution was selected for $Y_{i,t}$, as a heavy-tailed loss distribution was needed to account for the fact that individual claim amounts are positive and may include large outliers. That is,

$$\begin{aligned} N_t &\sim \text{Poisson}(\theta), \quad 0 < \theta < \infty, \\ Y_{i,t} &\sim \text{Pareto}(\alpha, \beta), \quad \alpha > 0, \quad 0 < \beta < y. \end{aligned}$$

The Pareto(α, β) distribution with support $[\beta, \infty)$ was particularly suitable in this context, as it was employed to model claim amounts exceeding a specified threshold.

In addition, the following assumptions were made:

- N_t are independently and identically distributed (i.i.d.) across t,
- $Y_{i,t}$ are i.i.d. across both i and t,
- N_t and $Y_{i,t}$ are independent for all i and t.

Under these assumptions, the aggregate claim amount in year t was defined as

$$S_t = Y_{1,t} + Y_{2,t} + \cdots + Y_{N_t,t}.$$

Next, prior distributions for the parameters α, β, and θ were specified. Due to limited prior knowledge about their true values—beyond the assumption that they are strictly positive—vague Gamma priors[2] were chosen:

$$\alpha \sim \text{Gamma}(1, 0.0001), \quad \beta \sim \text{Gamma}(1, 0.0001), \quad \theta \sim \text{Gamma}(1, 0.0001),$$

with the constraint $0 < \beta < \min\{y_{i,t}\}$ to ensure validity of the Pareto distribution.

Finally, the posterior distributions were derived. First, the joint posterior distribution of (α, β) was obtained via Bayes' theorem[3]:

$$\begin{aligned} \pi(\alpha, \beta \mid \mathbf{y}) &\propto \pi(\alpha) \cdot \pi(\beta) \cdot f(\mathbf{y} \mid \alpha, \beta) \\ &\propto 0.0001 \cdot \exp(-0.0001\alpha) \cdot 0.0001 \cdot \exp(-0.0001\beta) \cdot \prod_{i=1}^{n} \frac{\alpha \beta^{\alpha}}{y_i^{\alpha+1}} \\ &\propto \exp(-0.0001\alpha) \cdot \exp(-0.0001\beta) \cdot \alpha^n \cdot \beta^{n\alpha} \left(\prod_{i=1}^{n} y_i \right)^{-(\alpha+1)} \\ &\propto \alpha^n \cdot \exp(-0.0001\alpha) \cdot \left(\prod_{i=1}^{n} y_i \right)^{-\alpha} \cdot \beta^{n\alpha} \cdot \exp(-0.0001\beta) \\ &\propto \alpha^n \cdot \exp\left(- \left(0.0001 + \sum_{i=1}^{n} \ln(y_i) \right) \alpha \right) \cdot \beta^{n\alpha} \cdot \exp(-0.0001\beta) \end{aligned}$$

As a result, the full conditional posterior distributions of α and β were as follows:

$$\begin{aligned} \pi(\alpha \mid \beta, \mathbf{y}) &\propto \alpha^n \cdot \exp\left(- \left(0.0001 - n \ln(\beta) + \sum_{i=1}^{n} \ln(y_i) \right) \alpha \right), \\ \pi(\beta \mid \alpha, \mathbf{y}) &\propto \beta^{n\alpha} \cdot \exp(-0.0001\beta), \end{aligned}$$

which implied that:

$$\begin{aligned} \alpha \mid \beta, \mathbf{y} &\sim \text{Gamma}\left(n + 1, \sum_{i=1}^{n} \ln(y_i) - n \ln(\beta) + 0.0001 \right), \\ \beta \mid \alpha, \mathbf{y} &\sim \text{Gamma}(n\alpha + 1, 0.0001). \end{aligned}$$

[2] Each of these Gamma priors has a variance of 10^8, implying minimal prior influence so that most of the information about the parameters is derived from the dataset. Additionally, the Gamma distribution is conjugate to both the Poisson and Pareto likelihoods, facilitating analytical tractability in Bayesian inference.

[3] Here, assuming that α and β are independent, the joint prior $\pi(\alpha, \beta)$ was computed as $\pi(\alpha) \cdot \pi(\beta)$.

Similarly, the posterior distribution of θ was obtained via Bayes' theorem:

$$\begin{aligned}\pi(\theta \mid \mathbf{n}) &\propto \pi(\theta) \cdot f(\mathbf{n} \mid \theta) \\ &\propto \exp(-0.0001\theta) \cdot \prod_{t=1}^{T} (\theta^{n_t} \cdot \exp(-\theta)) \\ &\propto \exp(-0.0001\theta) \cdot \theta^{\sum_{t=1}^{T} n_t} \cdot \exp(-5\theta) \\ &\propto \exp(-5.0001\theta) \cdot \theta^{\sum_{t=1}^{T} n_t}\end{aligned}$$

which implied that:

$$\theta \mid \mathbf{n} \sim \text{Gamma}\left(\sum_{t=1}^{T} n_t + 1, 5.0001\right)$$

3.2 Gibbs Sampling Results

Since all three posterior distributions were standard distributions, the Gibbs sampling method was employed to draw realizations from them[4]. This was implemented using the `JAGS` program, which was called from within `R`. Following Dudley (2006), three Markov chains were run in parallel. The initial values of α, β, and θ were chosen to be well-dispersed and are presented in Table 2.

Table 2: Initial Parameter Values

Chain	α	β	θ
1	1×10^{-5}	1×10^{-5}	1×10^{-5}
2	1×10^{5}	1	1×10^{5}
3	3.076	1.625	3.200

These initial values are taken from Dudley (2006).

A burn-in of 20,000 iterations was used. The statistics computed from the subsequent 30,000 iterations are presented in Table 3. A comparison with those reported by Dudley (2006) shows a close match, indicating that the model was properly specified and the Gibbs sampler executed correctly.

Table 3: Posterior Statistics

	Mean	**Standard Deviation**	**95% Bayesian Credible Interval**
α	3.079	0.763	(1.771, 4.741)
β	1.592	0.035	(1.498, 1.624)
θ	3.396	0.821	(1.982, 5.192)
$E[Y]$	2.499	0.621	(2.024, 3.621)

$E[Y]$ was calculated for each simulated set of parameters α and β, and from these values, the mean, standard deviation, and 95% Bayesian credible interval were subsequently computed.

In addition, density plots were generated for each of the parameters and for $E[Y]$, as presented in Figure 1. The resulting densities for the parameters resemble Gamma distributions, with the density of β appropriately truncated at $\min\{y_{i,t}\} = 1.625$. The plot for $E[Y]$ displays a right-skewed distribution that permits very large values, albeit with very low probability—consistent with expectations.

The posterior means of α and β were used as parameters of the Pareto distribution, and the corresponding cumulative distribution function (CDF) was plotted against the empirical cumulative data ($y_{i,t}$). Similarly, the posterior mean of θ was used as the parameter of the Poisson distribution, and its CDF was plotted against the empirical cumulative data (n_t). The Pareto(3.079, 1.592) distribution provides a close fit to the empirical data. The Poisson(3.396) distribution also fits the observed frequencies quite well (see Figures 2 and 3).

3.3 Convergence Diagnostics

Throughout all computations above, it was assumed that the Markov chains had converged to a stationary distribution after discarding the initial 20,000 iterations, following the approach of Dudley (2006). However, it was essential to verify that convergence had indeed occurred. The first method of assessment involved visual inspection[5]. Figure 4 presents trace plots for all three parameters, showing the sampled values across iterations. These plots indicate good mixing, suggesting that the chains have likely converged.

The convergence of the chains was also assessed using the Gelman–Rubin diagnostic. The diagnostic was applied to the post-burn-in iterations (20,001–50,000), and the results are summarized in Table 4.

[4]Markov Chain Monte Carlo (MCMC) methods, like Gibbs sampling, are used to draw samples from intractable posterior distributions. Gibbs sampling is efficient when full conditional posteriors are in closed form, often with conjugate priors. When posteriors

Figure 1: Posterior Densities

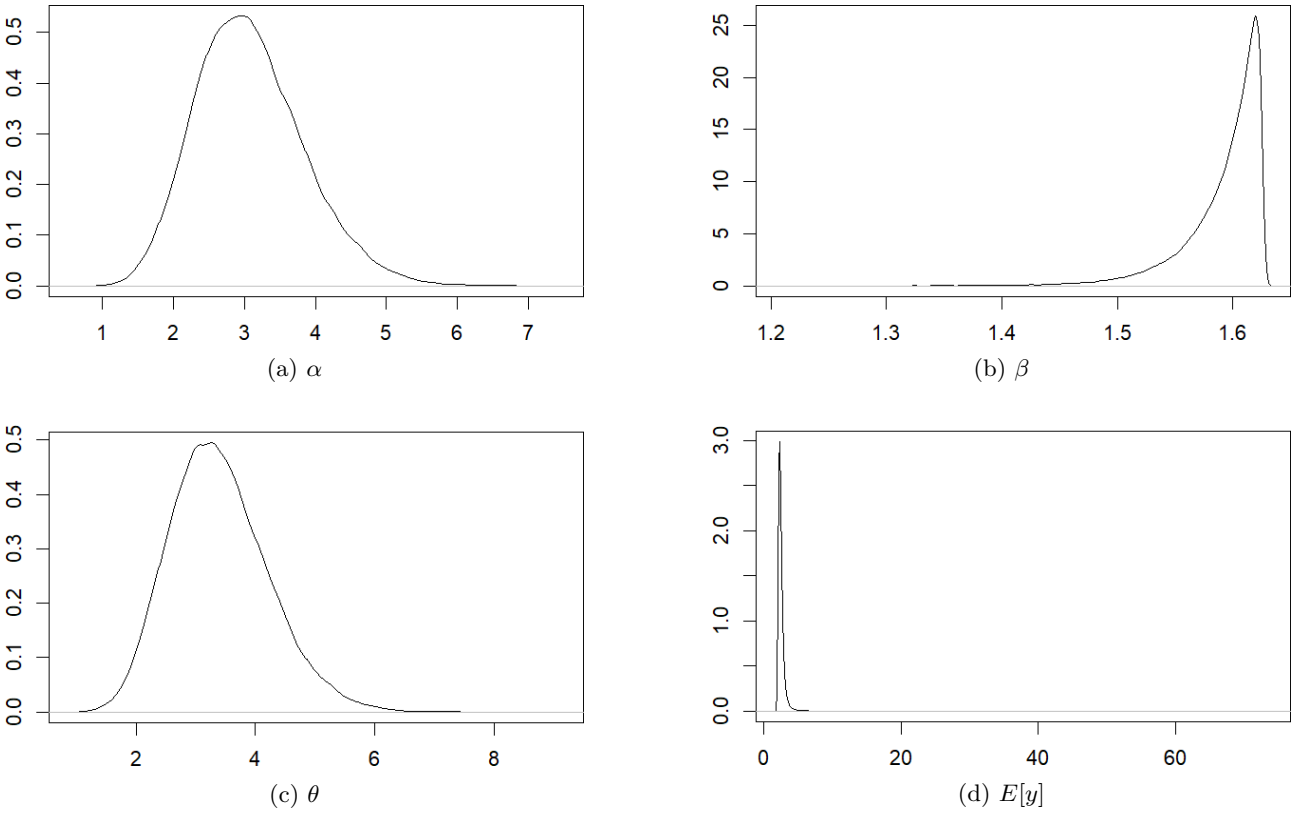

(a) α (b) β

(c) θ (d) $E[y]$

Figure 2: Empirical vs. Fitted Pareto CDF

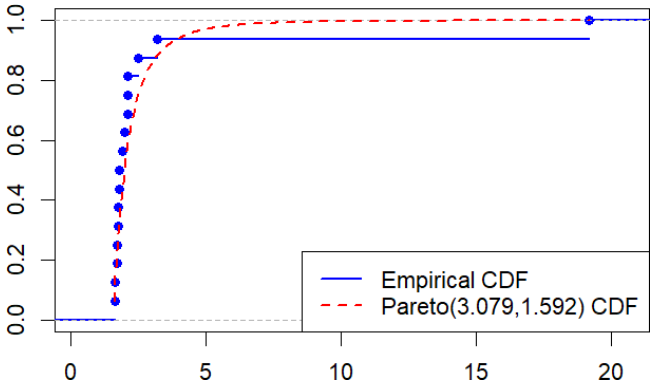

Figure 3: Empirical vs. Fitted Poisson CDF

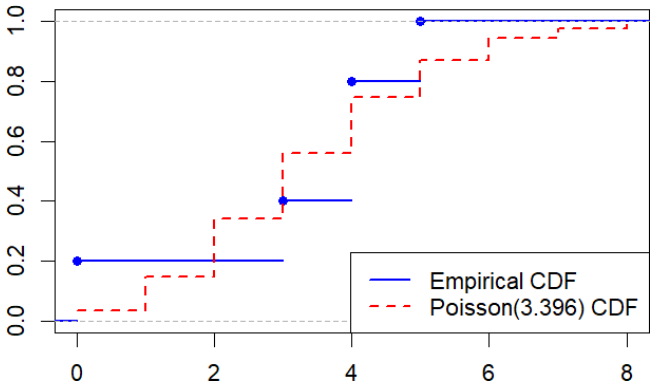

are not in closed form, the Metropolis-Hastings algorithm can be used to generate candidate values from a proposal distribution.

[5]Visual inspection involves assessing how well a chain explores the parameter space. Poor mixing—where the chain moves slowly or gets stuck—indicates potential convergence issues. Trace plots help identify such problems by showing how sampled values evolve

Figure 4: Trace Plots

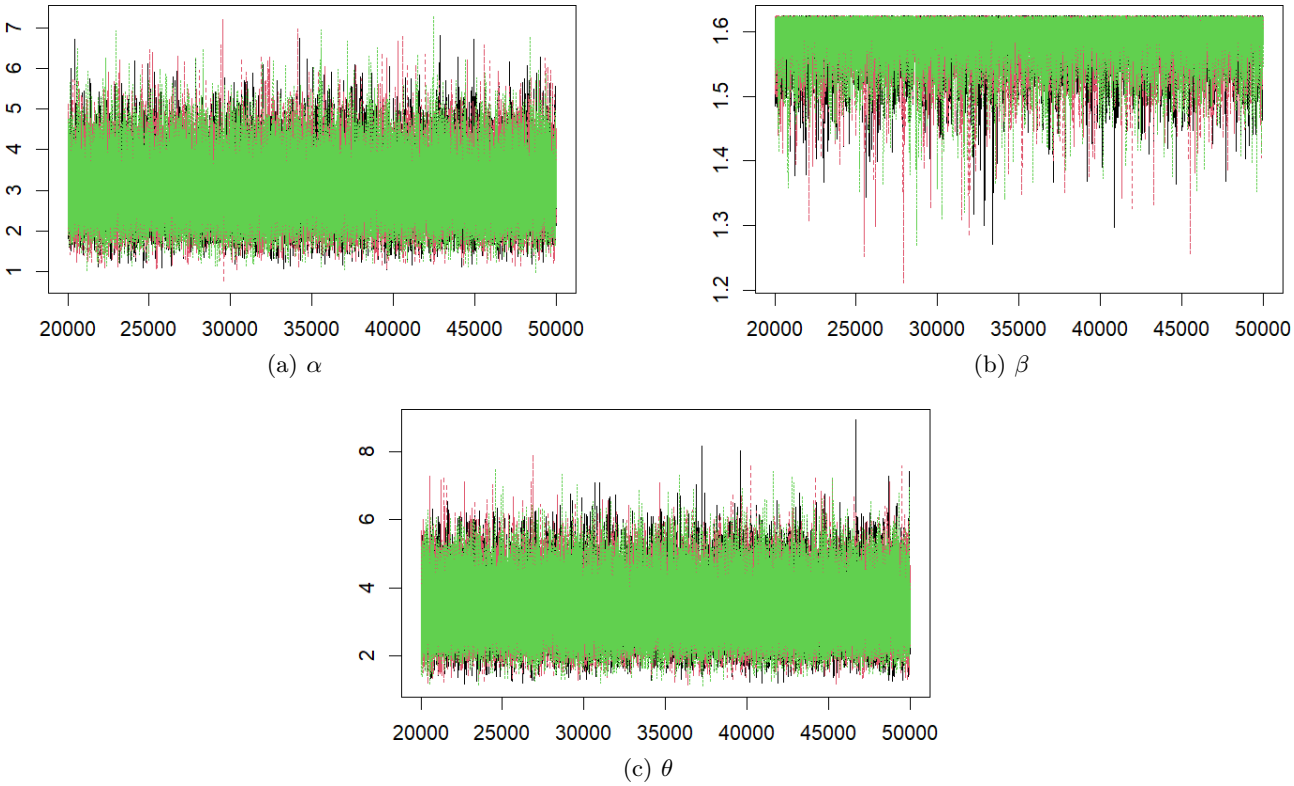

(a) α (b) β

(c) θ

Table 4: Potential Scale Reduction Factors (Gelman–Rubin Diagnostic)

Parameter	**Point Estimate**	**Upper C.I.**
α	1.00	1.00
β	1.00	1.00
θ	1.00	1.00
Multivariate PSRF	1.00	

All univariate potential scale reduction factors (PSRFs) have point estimates and upper confidence bounds at 1.00. The multivariate PSRF is also equal to 1.00. These values suggest that the Markov chains have likely converged, both for individual parameters and jointly.

Figure 5 shows how the univariate PSRF point estimates evolve with increasing iterations. Throughout all iterations, all estimates remain below 1.1, which is commonly considered an acceptable threshold for convergence. This further confirms that the chains have likely reached a stable distribution.

In addition, autocorrelation plots were generated for all three parameters (see Figure 6), and values at lags 1 through 10 are reported in Table 5. Several high autocorrelations were observed, particularly for β, which motivated the use of a thinning interval of 10 iterations, as suggested by Dudley.

Table 5: Autocorrelations at Lags 1–10

Lag	α	β	θ
1	0.297	0.705	0.003
2	0.119	0.509	0.005
3	0.061	0.373	−0.005
4	0.036	0.278	−0.004
5	0.023	0.210	0.001
6	0.016	0.161	−0.002
7	0.010	0.126	−0.004
8	0.009	0.102	−0.004
9	0.002	0.081	−0.001
10	0.007	0.065	0.004

Consequently, the chains were rerun with this thinning. Figure 7 presents the corresponding trace plots, and Figure 8 shows the updated autocorrelation plots. The trace plots indicate that the chains have mixed well, and all autocorrelation values at lags 2, 3, and beyond have become negligible.

over iterations for each parameter.

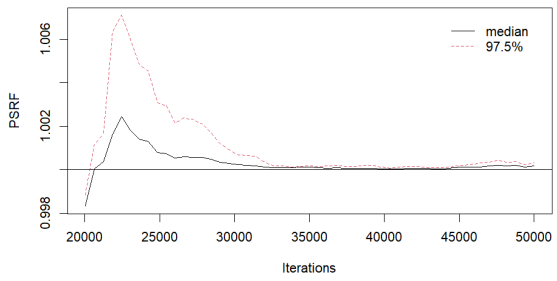

(a) α

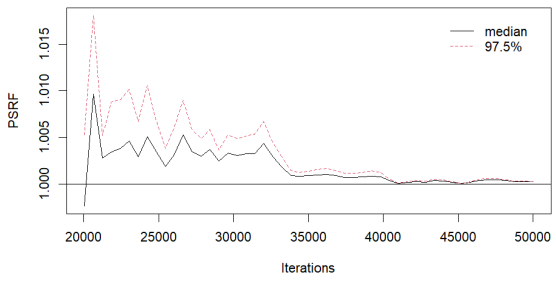

(b) β

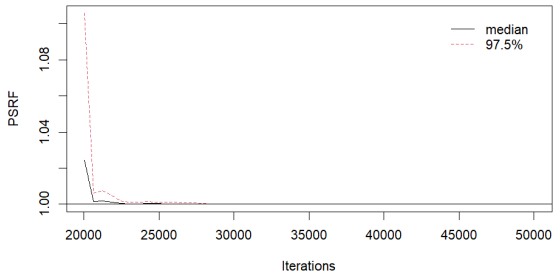

(c) θ

Figure 5: PSRF Values (Gelman–Rubin Diagnostic)

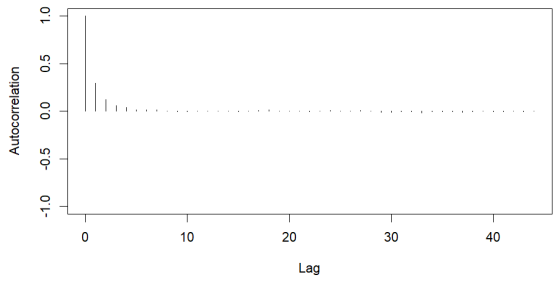

(a) α

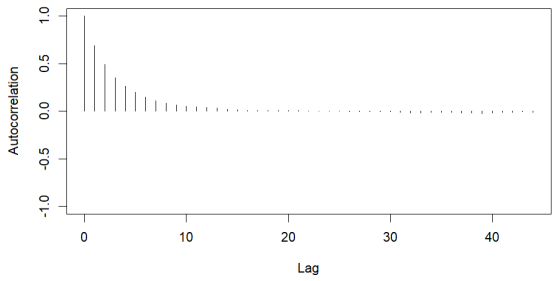

(b) β

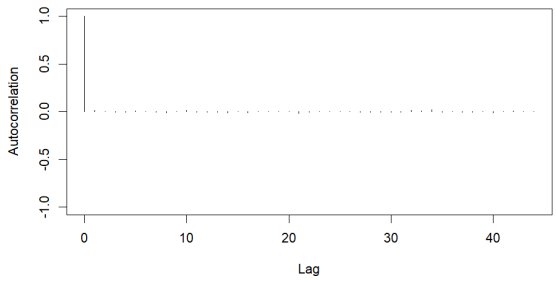

(c) θ

Figure 6: Autocorrelation Plots

Since the ultimate goal of the analysis was to predict the values of S_t, the posterior predictive distribution was employed. For a variable z, this distribution is defined as:

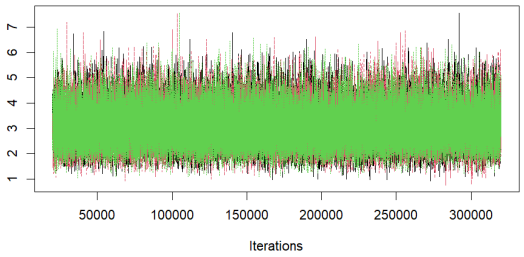

(a) α

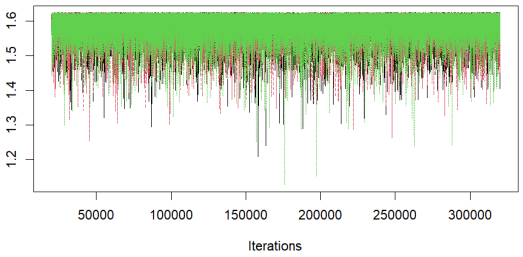

(b) β

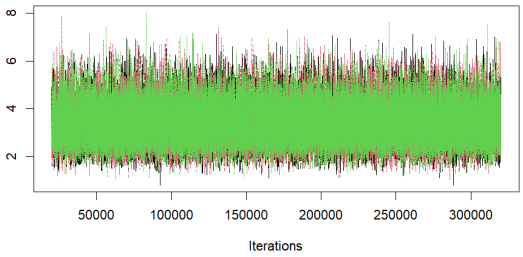

(c) θ

Figure 7: Trace Plots After Thinning

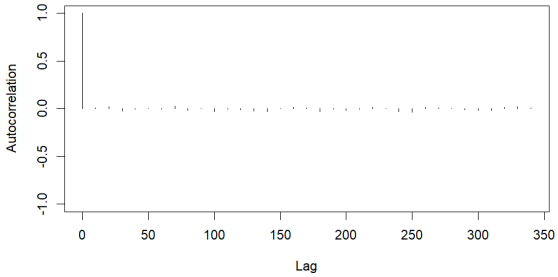

(a) α

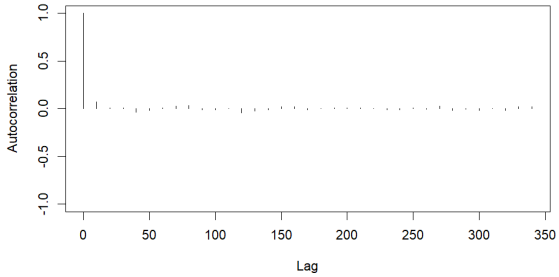

(b) β

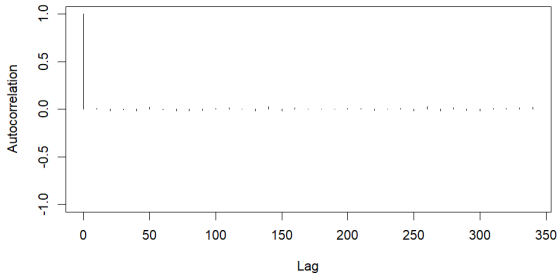

(c) θ

Figure 8: Autocorrelation Plots After Thinning

$$\pi(z \mid \mathbf{y}) = \int_{\Theta} f(z \mid \phi)\, \pi(\phi \mid \mathbf{y})\, d\phi$$

where $\phi = (\alpha, \beta, \theta)$, $\pi(\phi \mid \mathbf{y})$ is the posterior distribution of ϕ, and $f(z \mid \phi)$ is the likelihood of z given ϕ. This approach accounts for the uncertainty in ϕ by integrating over its possible values, weighted by their posterior

probabilities.

Let $\mathbf{n}$ denote the observed data and N_f represent a future observation. Then the posterior predictive distribution for N_f is:

$$\begin{aligned} p(N_f = n \mid \mathbf{n}) &= \int_0^\infty p(N_f = n \mid \theta)\pi(\theta \mid \mathbf{n})\, d\theta \\ &= \mathbb{E}_{\theta|\mathbf{n}}\left[p(N_f = n \mid \theta)\right] \\ &= \mathbb{E}_{\theta|\mathbf{n}}\left[\frac{\theta^n e^{-\theta}}{n!}\right] \end{aligned}$$

Since the integral could not be solved analytically, it was approximated using samples from the posterior distribution obtained via MCMC. Specifically, the expectation was approximated as:

$$p(N_f = n \mid \mathbf{n}) \approx \frac{1}{m}\sum_{i=1}^{m} \frac{(\theta^{(i)})^n e^{-\theta^{(i)}}}{n!} \tag{1}$$

where $\theta^{(i)}$ is the i-th sample from the MCMC chain and m is the number of iterations after burn-in and thinning.

Similarly, let $\mathbf{y}$ denote the observed data, and let Y_f represent a future observation. The posterior predictive cumulative distribution function (CDF) of Y_f is given by:

$$\begin{aligned} p(Y_f \le y \mid \mathbf{y}) &= \int_{\mathbf{u}} p(Y_f \le y \mid \mathbf{u})\, \pi(\mathbf{u} \mid \mathbf{y})\, d\mathbf{u} \\ &= \mathbb{E}_{\mathbf{u}|\mathbf{y}}\left[p(Y_f \le y \mid \alpha, \beta)\right] \end{aligned}$$

Again,

$$p(Y_f \le y \mid \mathbf{y}) \approx \frac{1}{m}\sum_{i=1}^{m}\left(1 - \left(\frac{\beta^{(i)}}{y}\right)^{\alpha^{(i)}}\right) \tag{2}$$

where $\alpha^{(i)}$ and $\beta^{(i)}$ denote the i-th samples from the MCMC chain, and m is the number of post-burn-in, thinned iterations.

Table 6 contains the estimated probabilities of $N_f = n$ for $n = 0, \ldots, 14$.

Table 6: Estimates of $p(N_f = n \mid \mathbf{n})$

n	Probability
0	0.0452
1	0.1279
2	0.1918
3	0.2023
4	0.1685
5	0.1178
6	0.0719
7	0.0393
8	0.0196
9	0.0091
10	0.0039
11	0.0016
12	0.0006
13	0.0002
14	0.0001

These results are consistent with those obtained by Dudley. As Y_f is a continuous variable, the probability density function (PDF) was estimated rather than discrete probabilities. The estimation employed the inverse cumulative distribution function (CDF) method.

A total of 1000 values $U \sim \text{Uniform}(0, 1)$ were generated. For each value, the transformation

$$y^{(i)} = \frac{\beta^{(i)}}{(1-U)^{1/\alpha^{(i)}}}$$

was applied. For each i, the mean of the resulting values was computed. The resulting values were then used to approximate the PDF of Y_f via kernel density estimation (KDE). The estimated predictive density is illustrated in Figure 9.

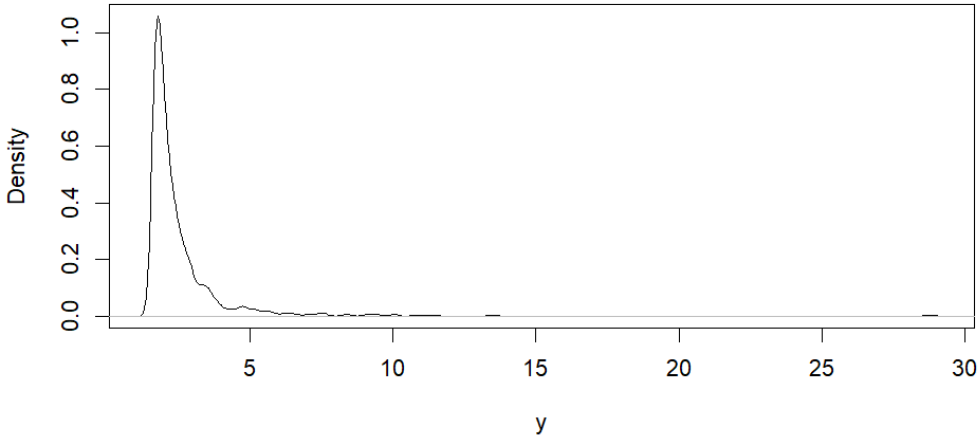

Figure 9: Estimated Predictive PDF of Y_f

The inverse CDF method was also used to estimate the predictive distribution of S_f, representing a future observation of S_t. The procedure was as follows: 1,000 values were drawn from the posterior predictive distribution of N_f. For each uniformly drawn U, a Poisson sample was generated using each posterior value of $\theta^{(i)}$, and the average of these samples was computed and rounded to obtain N_f. Then, for each simulated value of N_f, that many samples were drawn from the predictive distribution of Y_f (as described earlier), and the resulting values were summed to obtain a draw of S_f.

Figure 10 presents the histogram of the resulting S_f samples, along with the estimated density and three fitted distributions using moment matching. As observed by Dudley, the Gamma distribution provides the best fit. The fitted Gamma distribution has parameters $\alpha = 2.435$ and $\beta = 0.292$.

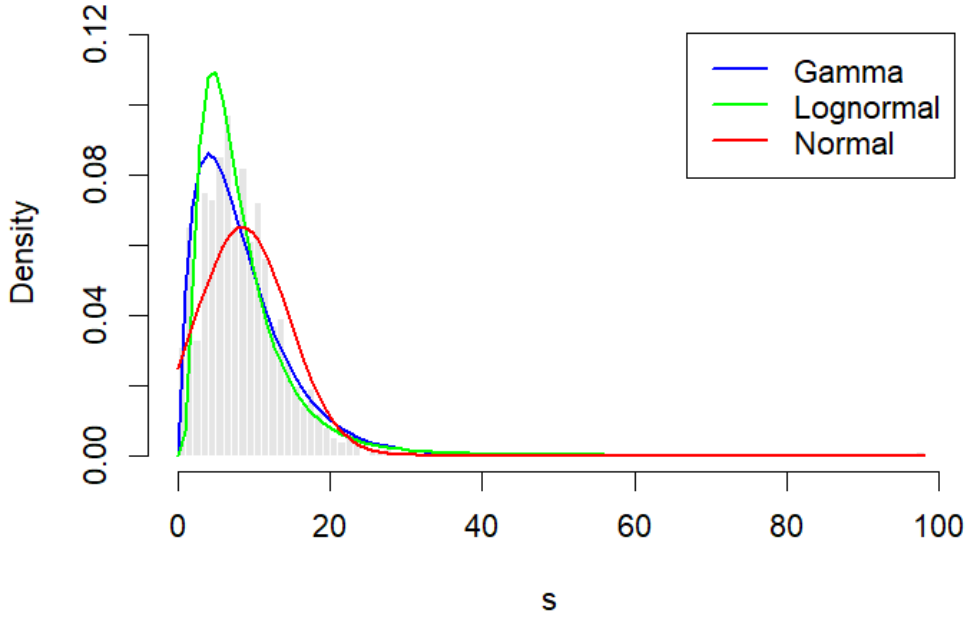

Figure 10: Histogram and Fitted Distributions for Predictive S_f

Table 7 shows various percentiles of the simulated S_f values. The distribution exhibits a suitably long tail, which aligns with expectations for a heavy-tailed claim size distribution. This indicates that the simulation method used was effective in generating large Y values, thereby capturing the tail behavior of the predictive

distribution of S more accurately. Proper representation of the tail is important, as most aggregate claims are moderate, but extreme values can occasionally occur.

Table 7: Percentiles of Simulated S_f Values

Percentile	**Value**
Median	7.630
90th Percentile	15.170
95th Percentile	18.103
99th Percentile	26.410
Maximum	35.851

References

Dudley, C. (2006). Bayesian Analysis of an Aggregate Claim Model Using Various Loss Distributions. Master's dissertation, Heriot-Watt University, School of Mathematical and Computer Sciences, Actuarial Mathematics & Statistics.

Rytgaard, M. (1990). Estimation in the Pareto Distribution. *ASTIN Bulletin*, 20(2):201–216.